Spatial-Frequency Block Coding Automatic Recognition with Non-Gaussian Interference for Cognitive MIMO-OFDM Systems

Junlin Zhang, Mingqian Liu, *Member, IEEE*, Yunfei Chen, *Senior Member, IEEE*, and Nan Zhao, *Senior Member, IEEE*

Abstract—**Space-time/frequency block coding (STBCs/SFBCs) scheme is a crucial technique for enhancing the effectiveness and reliability of multiple-input multiple-output orthogonal frequency-division multiplexing (MIMO-OFDM) systems with cognitive radio (CR) capability. Automatic recognition of STBCs/SFBCs is a prerequisite for achieving dynamic spectrum sharing in cognitive MIMO-OFDM systems. In contrast to existing works, this paper proposes a weighted cross-correlation function-based algorithm to recognize SFBCs for cognitive MIMO-OFDM systems with Gaussian noise and non-Gaussian impulsive interference. The proposed algorithm extracts the space-frequency redundancy information of different OFDM subcarriers on different receiver antenna pairs by using weighted cross-correlation functions. Then, the weighted cross-correlation feature vectors are constructed by exploiting the multi-antenna system so as to design the detection statistics and thresholds based on the central limit theorem. Finally, a decision tree method is adopted to discriminate between several SFBCs. The proposed algorithm does not require prior information such as channel coefficients, modulation schemes, noise power, or interference power. Simulation results show that the proposed algorithm is robust against non-Gaussian impulsive interference and achieves high recognition performance in the case of a small number of samples and a low signal-to-noise ratio.**

Index Terms—**Cognitive radio, multiple-input multiple-output, non-Gaussian impulsive interference, orthogonal frequency division multiplexing, parameter recognition, space-frequency block coding.**

I. Introduction

RAPID advancements in emerging technologies and services (e.g., mobile internet, Internet of things, big data, and robotics) have led to the proliferation of various devices and systems [1]. Hence, the problems of low spectrum efficiency, strong frequency-selective fading, and low transmission rates are becoming increasingly severe in wireless communication [2], [3]. In order to solve the spectrum insufficiency problem, cognitive radio (CR) is envisioned as a promising paradigm that provides a novel dynamic spectrum sharing strategy [4], [5]. This strategy facilitates the learning and perception of the radio environment (i.e., spectrum sensing, channel estimation, and communication parameter identification) and allows for the dynamic sharing of the licensed spectrum through the adjustment of the communication parameters [6]–[8]. It allows secondary users (SUs) to opportunistically utilize the licensed spectrum without affecting the Primary Users (PUs), thereby significantly improving the spectrum utilization efficiency. Recently, CR in conjunction with multiple-input multiple-output (MIMO) orthogonal frequency-division multiple (OFDM) access has received considerable attention as a candidate technology for future cognitive radio networks. The cognitive MIMO-OFDM system effectively fuses the advantages of MIMO and OFDM systems: MIMO technology makes full use of the space multiplexing gain, while OFDM technology can resist frequency-selective fading and suppress inter-symbol interference [9]–[12]. Accordingly, it allows for high-dimensional reuse of the licensed spectrum in the space, time, and frequency domains, thereby alleviating the challenge of scarce spectrum resources. It also fully exploits the advantages of the MIMO-OFDM antenna array to enhance the resistance to frequency-selective fading and inter-symbol interference. As an intelligent radio paradigm, cognitive MIMO-OFDM systems are also capable of learning from the radio environment(i.e., spectrum sensing, channel estimation, and communication parameter recognition) and adaptively modifying their transmission parameters in accordance with the learning results during their transmissions [13]. For MIMO-OFDM systems, the pace-time/frequency block coding is a critical communication parameter, which can effectively enhance the validity and reliability of data transmission. Hence, the recognition of space-time/frequency block coding (STBCs/SFBCs) is a key technology component in cognitive MIMO-OFDM systems. To further extend the application of cognitive radio in the context of non-cooperative communication, it is significant for secondary users to be capa-

This work was supported by the National Natural Science Foundation of China under Grant 62301380, 62071364 and 62231027, in part by the Natural Science Basic Research Program of Shaanxi under Grant 2024JC-JCQN-63, in part by the China Postdoctoral Science Foundation under Grant 2022M722504, in part by the Postdoctoral Science Foundation of Shaanxi Province under Grant 2023BSHEDZZ169, in part by the Key Research and Development Program of Shaanxi under Grant 2023-YBGY-249, in part by the Guangxi Key Research and Development Program under Grant 2022AB46002, in part by the Fundamental Research Funds for the Central Universities under Grant XJSJ23090 and Innovation Capability Support Program of Shaanxi under Grant 2024RS-CXTD-01. *(Corresponding author: Mingqian Liu.)*

J. Zhang and M. Liu are with the State Key Laboratory of Integrated Service Networks, Xidian University, Shaanxi, Xi'an 710071, China (e-mail: zhangjunlin@xidian.edu.cn; mqliu@mail.xidian.edu.cn).

Y. Chen is with Department of Engineering, University of Durham, Durham, UK DH1 3LE (e-mail: Yunfei.Chen@durham.ac.uk).

N. Zhao is with the School of Information and Communication Engineering, Dalian University of Technology, Dalian 116024, China (e-mail: zhaonan@dlut.edu.cn).

TABLE I
THE MAIN SYMBOLS IN THIS PAPER

Symbols	Explanation
M_t	Transmit antennas
M_r	Receive antennas
N_z	The number of OFDM subcarriers
ν	The length of cyclic prefix
$\mathbf{x}_b$	The data block
$\mathbf{C}(\mathbf{x}_b)$	The encoding matrix
$\mathbf{H}_k$	The channel matrix
$\mathbf{y}_k(n)$	The received signal vector on the kth subcarrier
$\mathbf{s}_k(n)$	The transmitted signal vector
$\mathbf{w}_k(n)$	The frequency-domain Gaussian white noise
$\mathbf{I}_k(n)$	The frequency-domain alpha-stable interference
$J^{(i_1,i_2)}(k_1,k_2)$	The weighted cross-correlation
$\omega_{k_l}^{i_j}(n)$	The adaptive weighting coefficient
Υ	The set of receive antenna pairs
$\mathbf{J}_{\mathbf{C}}(k_1,k_2)$	The absolute value feature vectors
$\mathbf{Z}_{\mathbf{C}}(k_1,k_2)$	The exponential feature vectors
$T_{\mathbf{F}}$	The detection statistic
$\Psi_{\mathbf{F}}^{C_1}$	The detection threshold
$\mathcal{C}$	The SFBCs scheme candidate pooling
$\mu_{T_{\mathbf{F}}\mid\mathcal{H}_0}$	The mean of $T_{\mathbf{F}}$ under the $\mathcal{H}_0$ hypothesis
$\sigma^2_{T_{\mathbf{F}}\mid\mathcal{H}_0}$	The variance of $T_{\mathbf{F}}$ under the $\mathcal{H}_0$ hypothesis

TABLE II
THE MAIN NOTATIONS IN THIS PAPER

Notations	Descriptions
$[\cdot]^{\mathrm{T}}$	Transposition
$\lvert\cdot\rvert$	Absolute value
$(\cdot)^*$	Complex conjugate
$\mathbb{E}\{\cdot\}$	Mathematical expectation
lg	Base-10 logarithm
$\circ$	the Hadamard product
$\exp(\cdot)$	Exponential function
$\lVert\cdot\rVert_{\mathrm{F}}$	Frobenius norm
δ	Kronecker delta
$\Gamma(\cdot)$	Gamma Function
$\lVert\cdot\rVert_{l_1}$	l_1 norm
$\Pr(\mathrm{C})$	Probability of the event C
$\approx$	Approximately equal sign

ble of STBCs/SFBCs recognition. Specifically, the cognitive user is equipped with STBCs/SFBCs recognition feature to precisely regulate the transmission parameters to match the duration of the spectrum hole so as to avoid interference to the primary user. Consequently, we are motivated to investigate the issue of STBCs/SFBCs recognition for cognitive MIMO-OFDM systems.

A. Related Work

The problem of STBCs/SFBCs recognition refers to the process of identifying space multiplexing, space-time grouping coding, or space-frequency grouping coding under unknown or partially known parameters. For spatial encoding recognition algorithms in single-carrier MIMO systems, the maximum-likelihood-based (LFB) algorithm [14], the statistics correlation-based (SCB) algorithm [15]–[20], the cyclostationary-based (CCB) algorithm [21]–[23] and the Kolmogorov-Smirnov tests-based (KSB) algorithm [24], [25] were proposed. The LFB algorithm transforms the STBC recognition problem into a multi-hypothesis testing problem. It constructs a cost function using the likelihood function of the received signal and solves for the recognition of spatial encoding types through optimization. This method achieves good recognition performance when there is sufficient prior information but has high computational complexity. The SCB algorithm utilizes statistical quantities of the received signal (such as correlation functions, temporal correlation, higher-order statistics, etc.) to construct recognition feature sequences and design a classifier to perform recognition. This method exhibits good recognition performance at medium to high signal-to-noise ratios and has low computational complexity. The CCB algorithm analyzes cyclostationary statistics of the received signal, including second-order cyclostationary statistics and fourth-order cyclostationary statistics, to construct discriminating features. Then, the feature classifier is designed to enhance the recognition performance at the cost of computational complexity, particularly in low signal-to-noise conditions. The KSB algorithm formulates the STBCs recognition problem as a goodness-of-fit test. It uses the maximum distance between the empirical cumulative distribution functions (CDFs) of two statistical quantities in the received signal as a discriminating feature and employs the K-S test for decision-making. This method can also achieve good recognition performance at low signal-to-noise ratios but recognizes fewer types.

For mulit-carrier systems or MIMO-OFDM systems, several researches have been conducted. In [26], Eldemerdash *et al.* exploited the statistical properties by designing a new cross-correlation function of the MIMO-OFDM signal to identify spatial multiplexing (SM) and Alamouti (AL) codes. The algorithm does not require a priori information such as modulation format, noise power, or timing error. In [27], Karami *et al.* proposed a new identification algorithm based on second-order cyclostationary characteristics to distinguish AL-OFDM and SM-OFDM. The algorithm is robust to phase noise and timing offset. In [28], the cross-correlation of the received signals was extracted from different receiving antennas as identification features and binary hypothesis testing was performed to identify three different space-time encoding types. Marey *et al*. proposed an identification method based on hypothesis testing to distinguish AL signals and SM signals by analyzing the cross-correlation functions between different received antenna signals in [29]. In [30], discriminant feature vectors were constructed by using the signal subspace and noise subspace of adjacent subcarriers in OFDM. As a result, the decision tree based on a special distance criterion was employed to identify the space-frequency block coding. Gao *et al*. utilized the two-dimensional space-frequency redundancy of SFBC-OFDM and proposed two identification methods, namely the hypothesis testing-based method and the support-vector-machine-based method [31]. Both methods achieve good identification performance under a low signal-to-noise ratio. All the aforementioned methods assume that the environmental noise is Gaussian.

B. Contributions

With the ever-increasing occurrence of man-made electromagnetic interference and multiuser interference in wireless communication, the non-Gaussian nature of noise/interference is prevalent [32], [33]. These include power line systems, aviation communication, high-speed rail communication, and underwater communication [34], [35]. As the energy of impulsive interference is much greater than that of the background noise, this may affect users in cognitive MIMO-OFDM systems. Therefore, this study investigates the SFBCs recognition for cognitive MIMO-OFDM systems under non-Gaussian impulsive interference.

We propose a novel recognition method based on weighted cross-correlation functions. Based on the analysis of weighted cross-correlation functions for space-frequency encoding, the detection statistic and detection threshold are constructed using the weighted cross-correlation feature matrix. Further, a decision tree method is adopted to identify SFBCs. The main contributions of this paper are as follows.

- Different from existing works, we develop an effective algorithm for discriminating between several SFBCs schemes with Gaussian noise and $S\alpha S$ interference for the first time. Specifically, a weighted cross-correlation function is designed to recognize the SFBCs scheme candidate pooling (SM, AL, SF3, SF4) in cognitive MIMO-OFDM systems.
- We analyze the weighted cross-correlation function of different SFBCs schemes in MIMO-OFDM systems. Then, the multi-antenna receivers' characteristics are utilized to construct the absolute value feature vectors and the exponential feature vectors based on the weighted cross-correlation function. Using two types of feature matrices to construct a detection statistic transforms the problem of SFBCs recognition into a serial binary hypothesis testing problem.
- The proposed method does not require prior information such as the baseband modulation scheme, channel coefficients, noise power, and interference power. This method can effectively identify the SFBCs under non-Gaussian noise interference and frequency-selective fading, and it achieves good recognition performance in the case of a small number of samples and a low signal-to-noise ratio.

The organization of this paper is as follows. Section II introduces the system model. Section III describes the weighted cross-correlation function of SFBC-OFDM signals. Section IV discusses the proposed recognition scheme. Section V presents the simulation result. Finally, the paper is concluded in Section VI. Table I and Table II list the main symbols and notations in this paper, respectively.

II. System Model

Without loss of generality, consider a cognitive MIMO-OFDM system, which consists of a primary user (PU), a primary user base station, a cognitive radio base station, and a secondary user (SU). A typical scenario is illustrated in Fig. 1. Once the PU begins to communicate, the surrounding SU can learn and perceive the radio environment, including spectrum sensing, channel estimation, and communication parameter recognition. We assume PU is equipped with M_t transmit antennas, and SU has M_r receive antennas, N_z subcarriers and ν cyclic prefix samples for OFDM. At the transmitter, the transmitted symbols are first mapped using either M-ary phase shift keying (M-PSK) or M-ary quadrature amplitude modulation (M-QAM). Then, the modulated symbols are divided into blocks $\mathbf{x}_b$ of length N_s, with $\mathbf{x}_b = [x_{b,0}, x_{b,1}, \cdots, x_{b,N_s-1}]$. The SFBC encoder maps the rows of the encoding matrix $\mathbf{C}(\mathbf{x}_b)$ into L consecutive OFDM subcarriers. Commonly used SFBCs schemes include SM, AL, SF3, and SF4 [31]; their code matrices are given by

$$\mathbf{C}^{\mathrm{SM}}(\mathbf{x}_b) = [x_{b,0}, \cdots, x_{b,M_t-1}]^T, \tag{1}$$

$$\mathbf{C}^{\mathrm{AL}}(\mathbf{x}_b) = \begin{bmatrix} x_{b,0} & x_{b,1} \\ -x_{b,1}^* & x_{b,0}^* \end{bmatrix}^T, \tag{2}$$

$$\mathbf{C}^{\mathrm{SF3}}(\mathbf{x}_b) = \begin{bmatrix} x_{b,0} & x_{b,1} & \frac{x_{b,2}}{\sqrt{2}} \\ -x_{b,1}^* & x_{b,0}^* & \frac{x_{b,2}}{\sqrt{2}} \\ \frac{x_{b,2}^*}{\sqrt{2}} & \frac{x_{b,2}^*}{\sqrt{2}} & \frac{-x_{b,0}-x_{b,0}^*+x_{b,1}-x_{b,1}^*}{2} \\ \frac{x_{b,2}^*}{\sqrt{2}} & -\frac{x_{b,2}^*}{\sqrt{2}} & \frac{x_{b,1}+x_{b,1}^*+x_{b,0}-x_{b,0}^*}{2} \end{bmatrix}^T \tag{3}$$

$$\mathbf{C}^{\mathrm{SF4}}(\mathbf{x}_b) = \begin{bmatrix} x_{b,0} & x_{b,1} & x_{b,2} \\ -x_{b,1} & x_{b,0} & -x_{b,3} \\ -x_{b,2} & x_{b,3} & x_{b,0} \\ -x_{b,3} & -x_{b,2} & x_{b,1} \\ x_{b,0}^* & x_{b,1}^* & x_{b,2}^* \\ -x_{b,1}^* & x_{b,0}^* & -x_{b,3}^* \\ -x_{b,2}^* & x_{b,3}^* & x_{b,0}^* \\ -x_{b,3}^* & -x_{b,2}^* & x_{b,1}^* \end{bmatrix}^T. \tag{4}$$

Based on the principle of OFDM, the OFDM block undergoes an N_z-point inverse fast Fourier transform (IFFT) while simultaneously adding a cyclic prefix of length ν. At the receiver, assuming that the received signal has achieved time-frequency synchronization, the cyclic prefix is removed, and the OFDM symbols are demodulated by performing an

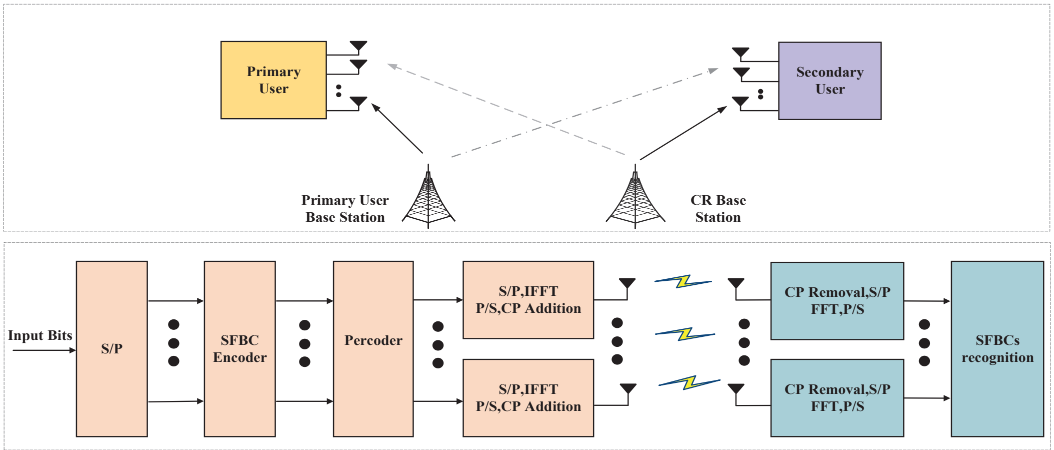

Fig. 1. Block diagram of the SFBCs recognition for cognitive MIMO-OFDM systems.

N_z-point FFT. The transmission channel is regarded as a frequency-selective fading channel, and the channel matrix can be defined as

$$\mathbf{H}_k = \begin{bmatrix} H^{(1,1)} & \cdots & H^{(M_t,1)} \\ \vdots & \ddots & \vdots \\ H^{(1,M_r)} & \cdots & H^{(M_t,M_r)} \end{bmatrix}, \tag{5}$$

where $H^{(f_i,f_j)}$ represents the kth subchannel coefficient between the f_ith transmit antenna and the f_jth receive antenna. The nth received signal of the kth OFDM subcarrier can be denoted as

$$\begin{aligned} \mathbf{y}_k(n) &= \tilde{\mathbf{s}}_k(n) + \mathbf{I}_k(n) + \mathbf{w}_k(n) \\ &= \mathbf{H}_k \mathbf{s}_k(n) + \mathbf{I}_k(n) + \mathbf{w}_k(n), \end{aligned} \tag{6}$$

where $\mathbf{y}_k(n)$ represents the received signal vector on the kth subcarrier, $\mathbf{s}_k(n)$ represents the transmitted signal vector, $\mathbf{w}_k(n)$ denotes the Gaussian white noise on the kth subcarrier, and $\mathbf{I}_k(n)$ represents the n-th non-Gaussian impulsive interference on the kth subcarrier. The impulsive interference follows a symmetric alpha stable ($S\alpha S$) distribution. Specifically, the $S\alpha S$ distribution is described by its characteristic function as

$$\varphi(I) = e^{(je_\alpha I - \gamma_\alpha |I|^\alpha)}, \tag{7}$$

where e_α is the location parameter, γ_α denotes the scale parameter, and $\alpha \in [1,2)$ represents the characteristic exponent, which controls the heaviness of the tails of the impulsive interference. The smaller the value of α is, the heavier the impulsive are [35].

III. Weighted Cross-Correlation Function of SFBC-OFDM Signals

To address the recognition problem of the SFBCs scheme in complex noisy environments, we propose a recognition algorithm based on the weighted cross-correlation function (WCCF). First, according to [31], [36], the weighted cross-correlation function $J^{(i_1,i_2)}(k_1,k_2)$ can be defined as

$$J^{(i_1,i_2)}(k_1,k_2) = \mathbb{E}\left\{ \frac{y_{k_1}^{i_1}(n)}{\omega_{k_1}^{i_1}(n)} \frac{y_{k_2}^{i_2}(n)}{\omega_{k_2}^{i_2}(n)} \right\}, \tag{8}$$

where $y_{k_l}^{i_j}(n)$ represents the k_lth OFDM subcarrier signal at the i_jth receiving antenna, and $\omega_{k_l}^{i_j}(n)$ denotes the adaptive weighting coefficient. $J^{(i_1,i_2)}(k_1,k_2)$ is considered to be extended from cross-correlation function by introducing $\omega_{k_l}^{i_j}(n)$. The adaptive weighting coefficient $\omega_{k_l}^{i_j}(n)$ is constructed constructed from the envelope of received signal $y_{k_l}^{i_j}$ and the second quartile of $\left|y_{k_l}^{i_j}(n)\right|$, which can be expressed as

$$\omega_{k_l}^{i_j}(n) = \begin{cases} 1 & \left|y_{k_l}^{i_j}(n)\right| \le q_{k_l}^{i_j} \\ \left[c_{k_l}^{i_j}(n)\right]^2 & \left|y_{k_l}^{i_j}(n)\right| > q_{k_l}^{i_j} \end{cases}, \tag{9}$$

where $c_{k_l}^{i_j}(n) = \left|y_{k_l}^{i_j}(n)\right| \big/ q_{k_l}^{i_j}$, $q_{k_l}^{i_j} = (1+2b_0)\, d_{k_l}^{i_j}$, b_0 represents a constant value ($b_0 > 0$), and $d_{k_l}^{i_j}$ denotes the second quartile of $\left|y_{k_l}^{i_j}(n)\right|$.

Assuming that the transmitted signals are independent and identically distributed, $\mathbb{E}\left\{x_{b,m} x_{b',m'}^*\right\} = \sigma_s^2 \delta(b-b')\,\delta(m-m')$, the Gaussian white noise $w_{k_l}^{i_j}(n)$ satisfies $\mathbb{E}\left\{w_{k_1}^{i_1}(n)\, w_{k_2}^{i_2}(n')\right\} =$

$$\begin{aligned} J^{(i_1,i_2)}(k_1,k_2) &= \mathbb{E}\left\{ \frac{y_{k_1}^{i_1}(n)\, y_{k_2}^{i_2}(n)}{\omega_{k_1}^{i_1}(n)\, \omega_{k_2}^{i_2}(n)} \right\} \\ &\approx \mathbb{E}\left\{ \frac{\tilde{s}_{k_1}^{i_1}(n)\, \tilde{s}_{k_2}^{i_2}(n)}{\omega_{k_1}^{i_1}(n)\, \omega_{k_2}^{i_2}(n)} \right\} + \mathbb{E}\left\{ \frac{I_{k_1}^{i_1}(n)\, I_{k_2}^{i_2}(n)}{\omega_{k_1}^{i_1}(n)\, \omega_{k_2}^{i_2}(n)} \right\} + \mathbb{E}\left\{ \frac{w_{k_1}^{i_1}(n)\, w_{k_2}^{i_2}(n)}{\omega_{k_1}^{i_1}(n)\, \omega_{k_2}^{i_2}(n)} \right\}. \end{aligned} \tag{10}$$

$\sigma_w^2\delta(i_1-i_2)\delta(k_1-k_2)\delta(n-n')$. In addition, the signals $s_{k_l}^{i_j}(n)$, the Gaussian noise $w_{k_l}^{i_j}(n)$, and non-Gaussian interference $I_{k_l}^{i_j}(n)$ are mutually uncorrelated. Based on these assumptions, we analyze WCCF between the k_1th OFDM subcarriers at the i_1 receive antenna and and k_2th OFDM subcarriers at the i_2th receive antenna. Using (6) and (8), $J^{(i_1,i_2)}(k_1,k_2)$ can be expressed as in (10) at the bottom of this page. Based on (9), when $\left|y_{k_1}^{i_1}(n)\right| \le q_{k_1}^{i_1}$ or $\left|y_{k_2}^{i_2}(n)\right| \le q_{k_2}^{i_2}$, it follows that $\omega_{k_l}^{i_j}(n)=1$. This implies that the amplitude of received signal $y_{k_l}^{i_j}(n)$ is less than a multiple of the second quartile of $\left|y_{k_l}^{i_j}(n)\right|$. In other words, the impulsive component of $y_{k_l}^{i_j}(n)$ is weak, i.e., signal $\tilde{s}_{k_1}^{i_1}(n)$ or $\tilde{s}_{k_2}^{i_2}(n)$ is affected only by small-amplitude interference represented by $I_{k_l}^{i_j}(n)$; hence, $\mathbb{E}\left\{I_{k_1}^{i_1}(n)I_{k_2}^{i_2}(n)\right\}<\infty, 1\le\alpha<2$. Therefore, $J^{(i_1,i_2)}(k_1,k_2)$ can be rewritten as

$$\begin{aligned}&J^{(i_1,i_2)}(k_1,k_2)\approx A_1\mathbb{E}\left\{\tilde{s}_{k_1}^{i_1}(n)\tilde{s}_{k_2}^{i_2}(n)\right\}\\&+A_1\mathbb{E}\left\{I_{k_1}^{i_1}(n)I_{k_2}^{i_2}(n)\right\}+A_1\mathbb{E}\left\{w_{k_1}^{i_1}(n)w_{k_2}^{i_2}(n)\right\},\end{aligned}\tag{11}$$

where A_1 represents a value that is dependent on $\omega_{k_l}^{i_j}(n)$. When the signal-to-noise ratio and signal-to-interference ratio are sufficiently high, (11) can be further approximated as

$$J^{(i_1,i_2)}(k_1,k_2)\approx A_1E\left\{\tilde{s}_{k_1}^{i_1}(n)\tilde{s}_{k_2}^{i_2}(n)\right\}.\tag{12}$$

If $\left|y_{k_l}^{i_j}(n)\right|>q_{k_l}^{i_j}$, considering the influence of impulsive interference from $I_{k_l}^{i_j}(n)$ on signal $s_{k_l}^{i_j}(n)$, it follows that $\omega_{k_l}^{i_j}(n)=\left[c_{k_l}^{i_j}(n)\right]^2$. In this case, $J^{(i_1,i_2)}(k_1,k_2)$ can be approximated as

$$\begin{aligned}J^{(i_1,i_2)}(k_1,k_2)&\approx\mathbb{E}\left\{\frac{\tilde{s}_{k_1}^{i_1}(n)\tilde{s}_{k_2}^{i_2}(n)}{\omega_{k_1}^{i_1}\omega_{k_2}^{i_2}}\right\}\\&+\mathbb{E}\left\{\frac{I_{k_1}^{i_1}(n)I_{k_2}^{i_2}(n)}{\omega_{k_1}^{i_1}\omega_{k_2}^{i_2}}\right\}+\mathbb{E}\left\{\frac{w_{k_1}^{i_1}(n)w_{k_2}^{i_2}(n)}{\omega_{k_1}^{i_1}\omega_{k_2}^{i_2}}\right\}\\&\approx\mathbb{E}\left\{\frac{\tilde{s}_{k_1}^{i_1}(n)\tilde{s}_{k_2}^{i_2}(n)}{\left(\left|y_{k_1}^{i_1}(n)\right|/q_{k_1}^{i_1}\right)^2\left(\left|y_{k_2}^{i_2}(n)\right|/q_{k_2}^{i_2}\right)^2}\right\}\\&+\mathbb{E}\left\{\frac{I_{k_1}^{i_1}(n)I_{k_2}^{i_2}(n)}{\left(\left|y_{k_1}^{i_1}(n)\right|/q_{k_1}^{i_1}\right)^2\left(\left|y_{k_2}^{i_2}(n)\right|/q_{k_2}^{i_2}\right)^2}\right\}\\&+\mathbb{E}\left\{\frac{w_{k_1}^{i_1}(n)w_{k_2}^{i_2}(n)}{\left(\left|y_{k_1}^{i_1}(n)\right|/q_{k_1}^{i_1}\right)^2\left(\left|y_{k_2}^{i_2}(n)\right|/q_{k_2}^{i_2}\right)^2}\right\}.\end{aligned}\tag{13}$$

For high signal-to-noise ratio, $J^{(i_1,i_2)}(k_1,k_2)$ can be approximated for independent and identically distributed strong impulsive interference as in (14) at the bottom of the page.

Setting $A_2=\mathbb{E}\left\{\frac{1}{\left(\left|y_{k_1}^{i_1}(n)\right|/q_{k_1}^{i_1}\right)^2\left(\left|y_{k_2}^{i_2}(n)\right|/q_{k_2}^{i_2}\right)^2}\right\}$, the expression of $J^{(i_1,i_2)}(k_1,k_2)$ can be rewritten as

$$\begin{aligned}&J^{(i_1,i_2)}(k_1,k_2)\\&\approx A_2\mathbb{E}\left\{\tilde{s}_{k_1}^{i_1}(n)\tilde{s}_{k_2}^{i_2}(n)\right\}+A_2\mathbb{E}\left\{w_{k_1}^{i_1}(n)w_{k_2}^{i_2}(n)\right\}\\&+\mathbb{E}\left\{\frac{I_{k_1}^{i_1}(n)I_{k_2}^{i_2}(n)}{\left(\left|y_{k_1}^{i_1}(n)\right|/q_{k_1}^{i_1}\right)^2\left(\left|y_{k_2}^{i_2}(n)\right|/q_{k_2}^{i_2}\right)^2}\right\}\\&\approx A_2\mathbb{E}\left\{\tilde{s}_{k_1}^{i_1}(n)\tilde{s}_{k_2}^{i_2}(n)\right\}.\end{aligned}\tag{15}$$

According to (12) and (15), $J^{(i_1,i_2)}(k_1,k_2)$ can be approximated as

$$J^{(i_1,i_2)}(k_1,k_2)\approx A_I\mathbb{E}\left\{\tilde{s}_{k_1}^{i_1}(n)\tilde{s}_{k_2}^{i_2}(n)\right\},\tag{16}$$

where A_I represents a value that is dependent on $\omega_{k_l}^{i_j}(n)$.

Based on the aforementioned discussions and the analysis presented in [31], the following conclusions can be drawn regarding various SFBC-OFDM signals.

$$\begin{aligned}J^{(i_1,i_2)}(k_1,k_2)\approx{}&\mathbb{E}\left\{\frac{1}{\left(\left|y_{k_1}^{i_1}(n)\right|/q_{k_1}^{i_1}\right)^2\left(\left|y_{k_2}^{i_2}(n)\right|/q_{k_2}^{i_2}\right)^2}\right\}\mathbb{E}\left\{\tilde{s}_{k_1}^{i_1}(n)\tilde{s}_{k_2}^{i_2}(n)\right\}\\&+\mathbb{E}\left\{\frac{1}{\left(\left|y_{k_1}^{i_1}(n)\right|/q_{k_1}^{i_1}\right)^2\left(\left|y_{k_2}^{i_2}(n)\right|/q_{k_2}^{i_2}\right)^2}\right\}\mathbb{E}\left\{w_{k_1}^{i_1}(n)w_{k_2}^{i_2}(n)\right\}+\mathbb{E}\left\{\frac{I_{k_1}^{i_1}(n)I_{k_2}^{i_2}(n)}{\left(\left|y_{k_1}^{i_1}(n)\right|/q_{k_1}^{i_1}\right)^2\left(\left|y_{k_2}^{i_2}(n)\right|/q_{k_2}^{i_2}\right)^2}\right\}.\end{aligned}\tag{14}$$

$$\begin{aligned}\mathbb{E}\left\{\tilde{s}_{k_1}^{i_1}(n)\tilde{s}_{k_2}^{i_2}(n)\right\}&=\mathbb{E}\left\{H_{k_1}^{(1,i_1)}H_{k_2}^{(1,i_2)}x_{b_1,0}x_{b_2,0}\right\}+\mathbb{E}\left\{H_{k_1}^{(1,i_1)}H_{k_2}^{(2,i_2)}x_{b_1,0}x_{b_2,1}\right\}\\&+\mathbb{E}\left\{H_{k_1}^{(2,i_1)}H_{k_2}^{(1,i_2)}x_{b_1,1}x_{b_2,0}\right\}+\mathbb{E}\left\{H_{k_1}^{(2,i_1)}H_{k_2}^{(2,i_2)}x_{b_1,1}x_{b_2,1}\right\}\\&=0.\end{aligned}\tag{17}$$

A. WCCF of SM-OFDM Signal

Assuming that at a given moment, the received symbols on different subcarriers k_1 and k_2 at different receiving antennas i_1 and i_2 are represented by $x_{b_1,0}$, $x_{b_1,1}$ and $x_{b_2,0}$, $x_{b_2,1}$, respectively, from the code matrix of SM in (1), can be derived (17) at the bottom of the page.

By substituting (17) into (16), we get

$$J_{\text{SM}}^{(i_1,i_2)}(k_1,k_2) \approx 0. \tag{18}$$

From (18), multiple consecutive OFDM sub-carriers in SM-OFDM signal are uncorrelated, so that $\left|J_{\text{SM}}^{(i_1,i_2)}(k_1,k_2)\right|$ does not exhibit peaks.

B. WCCF of AM-OFDM Signal

Using (2), assuming that at a given moment, the received symbols on different subcarriers k_1 and k_2 of different receiving antennas i_1 and i_2 are represented by $x_{b,0}$, $-x_{b,1}^*$ and $x_{b,1}$, $x_{b,0}^*$, respectively, based on the encoding matrix, it can be inferred that

$$\mathbb{E}\{\tilde{s}_k^{i_1}(n)\tilde{s}_{k+1}^{i_2}(n)\}=\left(H_k^{(1,i_1)}H_{k+1}^{(2,i_2)}-H_k^{(2,i_1)}H_{k+1}^{(1,i_2)}\right)\sigma_s^2. \tag{19}$$

From (16) and (19), we get

$$J_{\text{AL}}^{(i_1,i_2)}(k,k+1) \approx A_I R_2 \sigma_s^2, \tag{20}$$

where $R_2 = H_k^{(1,i_1)}H_{k+1}^{(2,i_2)} - H_k^{(2,i_1)}H_{k+1}^{(1,i_2)}$. In (20), the WCCF between OFDM subcarriers is not zero, so $\left|J_{\text{AL}}^{(i_1,i_2)}(k,k+1)\right|$ exhibits discriminating peaks.

C. WCCF of SF3-OFDM Signal

Using the code matrix of SF3 in (3), it can be derived that

$$\begin{aligned}\mathbb{E}\{\tilde{s}_k^{i_1}(n)\tilde{s}_{k+2}^{i_2}(n)\}=&\frac{\sigma_s^2}{2}\left(H_k^{(3,i_1)}H_{k+2}^{(1,i_2)}+H_k^{(3,i_1)}H_{k+2}^{(2,i_2)}\right)\\&-\frac{\sigma_s^2}{2}\left(H_k^{(1,i_1)}H_{k+2}^{(3,i_2)}+H_k^{(2,i_1)}H_{k+2}^{(3,i_2)}\right)\end{aligned} \tag{21}$$

Using (16) and (21), we can find that

$$J_{\text{SF3}}^{(i_1,i_2)}(k,k+2) \approx A_I R_3 \frac{\sigma_s^2}{2}, \tag{22}$$

where $R_3 = H_k^{(3,i_1)}H_{k+2}^{(1,i_2)} + H_k^{(3,i_1)}H_{k+2}^{(2,i_2)} - H_k^{(1,i_1)}H_{k+2}^{(3,i_2)} - H_k^{(2,i_1)}H_{k+2}^{(3,i_2)}$. According to (22), $\left|J_{\text{SF3}}^{(i_1,i_2)}(k,k+2)\right|$ provides a peak feature to discriminate the SF3.

D. WCCF of SF4-OFDM Signal

According to the code matrix of SF4 in (4), it can be shown that

$$\begin{aligned}&E\left\{\tilde{s}_k^{i_1}(n)\,\tilde{s}_{k+4}^{i_2}(n)\right\}\\&=\left(H_k^{(1,i_1)}H_{k+4}^{(2,i_2)}+H_k^{(2,i_1)}H_{k+4}^{(1,i_2)}+H_k^{(3,i_1)}H_{k+4}^{(3,i_2)}\right)\sigma_s^2,\end{aligned} \tag{23}$$

Relying on (16) and (23), one obtains

$$J_{\text{SF4}}^{(i_1,i_2)}(k,k+4) \approx A_I R_4 \sigma_s^2, \tag{24}$$

where $R_4 = H_k^{(1,i_1)}H_{k+4}^{(2,i_2)} + H_k^{(2,i_1)}H_{k+4}^{(1,i_2)} + H_k^{(3,i_1)}H_{k+4}^{(3,i_2)}$. As shown in (24), $\left|J_{\text{SF4}}^{(i_1,i_2)}(k,k+4)\right|$ exhibits the statistically significant peaks, which are exploited as a discriminating feature to identify SF4.

IV. Proposed SFBC-OFDM Classification Scheme

In practice, the WCCF is estimated as

$$\begin{aligned}\hat{J}^{(i_1,i_2)}(k_1,k_2) &= \frac{1}{N_b}\sum_{n=1}^{N_b}\frac{y_{k_1}^{i_1}(n)}{\omega_{k_1}^{i_1}(n)}\frac{y_{k_2}^{i_2}(n)}{\omega_{k_2}^{i_2}(n)}\\&= \tilde{J}_{\mathbf{C}}^{(i_1,i_2)}(k_1,k_2)+\varepsilon_J(k_1,k_2),\end{aligned} \tag{25}$$

where N_b represents the number of received OFDM symbols, $\tilde{J}_{\mathbf{C}}^{(i_1,i_2)}(k_1,k_2)$ is the weighted cross-correlation function of $\tilde{s}_{k_2}^{i_2}(n)$, $\varepsilon_J(k_1,k_2)$ denotes the estimation error, which includes the contribution of Gaussian noise and Non-Gaussian Interference, as well as the contribution of the estimation error that results due to using a finite length observation. When $N_b \to \infty$, $\varepsilon_J(k_1,k_2)$ takes on a very small value.

For a cognitive MIMO-OFDM system equipped with M_r antennas, the set of receive antenna pairs Υ can be defined as

$$\Upsilon = \{(i_1,i_2) : i_1 \neq i_2, 1 \leq i_1 \leq M_r, 1 \leq i_2 \leq M_r\}. \tag{26}$$

Using the set of receive antenna pairs Υ, the absolute value feature vectors $\mathbf{J_C}(k_1,k_2)$ and the exponential feature vectors $\mathbf{Z_C}(k_1,k_2)$ are constructed as in (27) and (28) at the bottom of the page. In (28), z_0 denotes a constant value ($z_0 > 0$).

First, the recognition algorithms for SM-OFDM and AL-OFDM are designed. Then, the recognition for other SFBC-OFDM schemes is analyzed. For both SM and AL, using (18), (20), and (25), we get

$$\begin{aligned}\hat{J}_{\text{SM}}^{(i_1,i_2)}(k,k+1) &= \tilde{J}_{\text{SM}}^{(i_1,i_2)}(k_1,k_2)+\varepsilon_J(k,k+1)\\&\approx \varepsilon_J(k,k+1),\end{aligned} \tag{29}$$

$$\begin{aligned}\hat{J}_{\text{AL}}^{(i_1,i_2)}(k,k+1) &= \tilde{J}_{\text{AL}}^{(i_1,i_2)}(k_1,k_2)+\varepsilon_J(k,k+1)\\&\approx A_I R_2 \sigma_s^2+\varepsilon_J(k,k+1).\end{aligned} \tag{30}$$

From (29) and (30), it is evident that when $N_b \to \infty$, $\left|\hat{J}_{\text{SM}}^{(i_1,i_2)}(k,k+1)\right|$ tends to an extremely small value while $\left|\hat{J}_{\text{AL}}^{(i,j)}(k,k+1)\right|$ exhibits significant non-zero peaks. Therefore, the recognition problem of SM-OFDM and AL-OFDM can be transformed into a binary hypothesis testing problem as

$$\left\{\begin{array}{l}\mathcal{H}_0 : \hat{J}^{(i_1,i_2)}(k,k+1) \approx \varepsilon_J(k,k+1)\\ \mathcal{H}_1 : \hat{J}^{(i_1,i_2)}(k,k+1) \approx A_I R_2 \sigma_s^2 + \varepsilon_J(k,k+1)\end{array}\right., \tag{31}$$

where $\mathcal{H}_0$ represents the hypothesis for SM and $\mathcal{H}_1$ represents the hypothesis for AL. For the aforementioned hypothesis testing problem, it is necessary to not only construct a detection statistic but also design detection thresholds.

Based on (27) and (28), the feature matrix $\mathbf{F}_{\mathbf{C}}^{k+1}$ can be defined as

$$\mathbf{F}_{\mathbf{C}}^{k+1} = \mathbf{J_C}(2j-1,2j) \circ \mathbf{Z_C}(2j-1,2j), \tag{32}$$

where "$\circ$" represents the Hadamard product, $j = 1, \cdots, L_{\max}^j$ ($L_{\max}^j$ denotes the maximum value of j, $j \in \Phi = \{1, \cdots k, \cdots, N_z\}$). From (32), $\mathbf{F}_{\mathbf{C}}^{k+1}$ is composed of the product of elements of $\mathbf{J_C}(k,k+1)$ and $\mathbf{Z_C}(k,k+1)$.

The detection statistic $T_{\mathbf{F}}$ can be constructed using the feature matrix $\mathbf{F}_{\mathbf{C}}^{k+1}$ as

$$T_{\mathbf{F}} = \frac{1}{L_{\mathbf{F}}^{k+1}}\left\|\mathbf{F}_{\mathbf{C}}^{k+1}\right\|_{l_1}, \tag{33}$$

where $L_{\mathbf{F}}^{k+1}$ represents the number of elements in matrix $\mathbf{F}_{\mathbf{C}}^{k+1}$ and $\|\cdot\|_{l_1}$ denotes the sum of the vector elements. The index $k+1$ indicates that the detection statistics is constructed from $J^{(i_1,i_2)}(k,k+1)$ between the k-th OFDM sub-carrier and $(k+1)$-th OFDM sub-carrier.

For the hypothesis testing in (31), the following decision rule is set based on the detection statistic as

$$\left\{ \begin{array}{l} \mathcal{H}_0 : T_{\mathbf{F}} \leq \Psi_{\mathbf{F}} \\ \mathcal{H}_1 : T_{\mathbf{F}} > \Psi_{\mathbf{F}} \end{array} \right. , \tag{34}$$

where $\Psi_{\mathbf{F}}$ represents the detection threshold. When the detection statistic $T_{\mathbf{F}}$ is less than the detection threshold $\Psi_{\mathbf{F}}$, the hypothesis $\mathcal{H}_0$ is accepted, indicating the result as SM-OFDM. Otherwise, the hypothesis $\mathcal{H}_1$ holds, indicating the result as AL-OFDM.

For SM-OFDM, when N_b is sufficiently large, it is assumed that $|\varepsilon_J(k,k+1)|$ approximately follows an Gaussian distribution. Therefore, $T_{\mathbf{F}}$ is also approximately Gaussian. The detection threshold $\Psi_{\mathbf{F}}$ can be set as

$$\Psi_{\mathbf{F}} = Q_{\mathbf{F}} \sigma_{T_{\mathbf{F}}|\mathcal{H}_0} + \mu_{T_{\mathbf{F}}|\mathcal{H}_0} , \tag{35}$$

where $\mu_{T_{\mathbf{F}}|\mathcal{H}_0}$ represents the mean of $T_{\mathbf{F}}$ under the $\mathcal{H}_0$ hypothesis, $\sigma^2_{T_{\mathbf{F}}|\mathcal{H}_0}$ represents the variance of $T_{\mathbf{F}}$ under the $\mathcal{H}_0$ hypothesis, and $Q_{\mathbf{F}}$ is the detection factor. However, at the receiver, it is not possible to know the mean and variance of $|\varepsilon_J(k,k+1)|$ in advance, which makes it impossible to directly calculate $\mu_{T_{\mathbf{F}}|\mathcal{H}_0}$ and $\sigma^2_{T_{\mathbf{F}}|\mathcal{H}_0}$. Therefore, it is necessary to estimate $\mu_{T_{\mathbf{F}}|\mathcal{H}_0}$ and $\sigma^2_{T_{\mathbf{F}}|\mathcal{H}_0}$.

For SM-OFDM and AL-OFDM, based on the encoding matrices, it can be determined as

$$\hat{J}_{\mathrm{SM}}^{(i_1,i_2)}(k,k+2) \approx \varepsilon_J(k,k+2) , \tag{36}$$

$$\hat{J}_{\mathrm{AL}}^{(i_1,i_2)}(k,k+2) \approx \varepsilon_J(k,k+2) , \tag{37}$$

where $\varepsilon_J(k,k+2)$ represents the error introduced by non-Gaussian noise interference and Gaussian noise, and it follows the same distribution as $\varepsilon_J(k,k+1)$. Therefore, $\hat{J}^{(i_1,i_2)}(k,k+2)$ can be used to estimate $\mu_{T_{\mathbf{F}}|\mathcal{H}_0}$ and $\sigma^2_{T_{\mathbf{F}}|\mathcal{H}_0}$. The error matrix $\tilde{\mathbf{F}}_{\mathbf{C}}^{k+2}$ is constructed using $\hat{J}^{(i_1,i_2)}(k,k+2)$ as

$$\tilde{\mathbf{F}}_{\mathbf{C}}^{k+2} = \mathbf{J}_{\mathbf{C}}(k,k+2) \circ \mathbf{Z}_{\mathbf{C}}(k,k+2) , \tag{38}$$

where $k = 1, \cdots, L_{\max}^k$($L_{\max}^k$ represents the maximum value of k). Based on the error matrix $\tilde{\mathbf{F}}_{\mathbf{C}}^{k+2}$, the estimated value $\hat{\mu}_{T_{\mathbf{F}}|\mathcal{H}_0}$ of $\mu_{T_{\mathbf{F}}|\mathcal{H}_0}$ can be calculated as

$$\hat{\mu}_{T_{\mathbf{F}}|\mathcal{H}_0} = \frac{1}{I_{\mathbf{F}}^{k+2}} \left\| \tilde{\mathbf{F}}_{\mathbf{C}}^{k+2} \right\|_{l_1} , \tag{39}$$

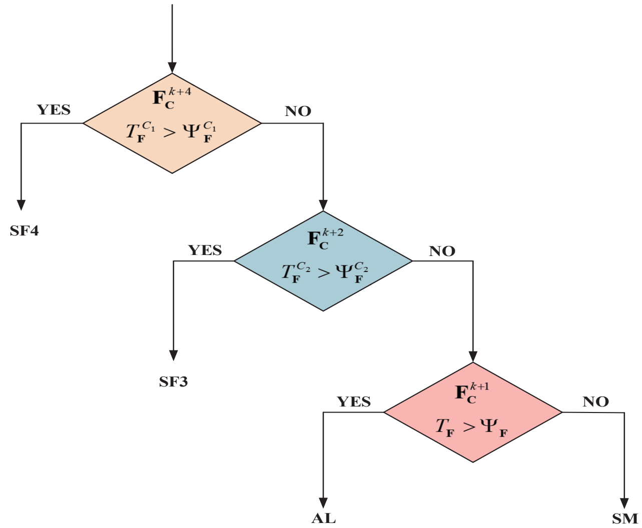

Fig. 2. Decision tree based on the WCCF for the recognition of SFBCs.

where $I_{\mathbf{F}}^{k+2}$ represents the number of elements in vector $\tilde{\mathbf{F}}_{\mathbf{C}}^{k+2}$. In addition, the values $\hat{\sigma}^2_{T_{\mathbf{F}}|\mathcal{H}_0}$ of $\sigma^2_{T_{\mathbf{F}}|\mathcal{H}_0}$ can be estimated as

$$\hat{\sigma}^2_{T_{\mathbf{F}}|\mathcal{H}_0} = \frac{1}{I_{\mathbf{F}}^{k+2}} \left(\frac{1}{I_{\mathbf{F}}^{k+2}} \left\| \tilde{\mathbf{F}}_{\mathbf{C}}^{k+2} \right\|_{l_1}^2 - \hat{\mu}^2_{T_{\mathbf{F}}|\mathcal{H}_0} \right) . \tag{40}$$

Therefore, the detection threshold $\Psi_{\mathbf{F}}$ can be further expressed as

$$\Psi_{\mathbf{F}} = Q_{\mathbf{F}} \hat{\sigma}_{T_{\mathbf{F}}|\mathcal{H}_0} + \hat{\mu}_{T_{\mathbf{F}}|\mathcal{H}_0} . \tag{41}$$

According to the decision criterion in (34), when $T_{\mathbf{F}} > \Psi_{\mathbf{F}}$, the received signal is classified as AL-OFDM. Otherwise, it is classified as SM-OFDM.

Based on the aforementioned recognition algorithm, a tree classification decision approach is designed for the target set $\Theta = \{$SM,AL,SF3,SF4$\}$, as shown in Fig.2.

In the first layer of the classification tree, we differentiate between SF4 and $\{$SM,AL,SF3$\}$. Based on the analysis in Section III, we observe that SF4 has a significant peak in $\hat{J}_C^{(i_1,i_2)}(k,k+4)$ compared to $\{$SM,AL,SF3$\}$. Therefore, we can use $\mathbf{J}_{\mathbf{C}}^{k+4}(k,k+4)$ to construct a statistical measure $T_{\mathbf{F}}^{C_1}$ for classification. The detection statistic $T_{\mathbf{F}}^{C_1}$ can be expressed as

$$T_{\mathbf{F}}^{C_1} = \frac{1}{L_{\mathbf{F}}^{k+4}} \left\| \mathbf{F}_{\mathbf{C}}^{k+4} \right\|_{l_1} , \tag{42}$$

where $L_{\mathbf{F}}^{k+4}$ represents the number of elements in matrix $\mathbf{F}_{\mathbf{C}}^{k+4}$, which can be expressed as in (43) at the bottom of

$$\mathbf{J}_{\mathbf{C}}(k_1,k_2) = \left[\left| \hat{J}^{(1,2)}(k_1,k_2) \right|, \left| \hat{J}^{(1,3)}(k_1,k_2) \right|, \cdots, \left| \hat{J}^{(M_r-1,M_r)}(k_1,k_2) \right| \right]^T , \tag{27}$$

$$\mathbf{Z}_{\mathbf{C}}(k_1,k_2) = \left[\exp\left(\frac{\left| \hat{J}^{(1,2)}(k_1,k_2) \right|}{z_0} \right), \cdots, \exp\left(\frac{\left| \hat{J}^{(M_r-1,M_r)}(k_1,k_2) \right|}{z_0} \right) \right]^T . \tag{28}$$

the page, where $\mathbf{B_C}(k_1,k_2)$ can be given by

$$\mathbf{B_C}(k_1,k_2)=\mathbf{J_C}(k_1,k_2)\circ\mathbf{Z_C}(k_1,k_2). \tag{44}$$

The detection threshold $\Psi_{\mathbf{F}}^{C_1}$ can be set as

$$\Psi_{\mathbf{F}}^{C_1}=Q_{\mathbf{F}}\hat{\sigma}_{T_{\mathbf{F}}^{C_1}|\mathcal{H}_0}+\hat{\mu}_{T_{\mathbf{F}}^{C_1}|\mathcal{H}_0}. \tag{45}$$

The estimation of $\hat{\mu}_{T_{\mathbf{F}}^{C_1}|\mathcal{H}_0}$ is given by the following expression as

$$\hat{\mu}_{T_{\mathbf{F}}^{C_1}|\mathcal{H}_0}=\frac{1}{I_{\mathbf{F}}^{k+9}}\left\|\tilde{\mathbf{F}}_{\mathbf{C}}^{k+9}\right\|_{l_1}, \tag{46}$$

where $I_{\mathbf{F}}^{k+9}$ represents the number of elements in matrix $\tilde{\mathbf{F}}_{\mathbf{C}}^{k+9}$. The estimated value $\hat{\sigma}^2_{T_{\mathbf{F}}^{C_1}|\mathcal{H}_0}$ of $\sigma^2_{T_{\mathbf{F}}^{C_1}|\mathcal{H}_0}$ can be obtained as

$$\hat{\sigma}^2_{T_{\mathbf{F}}^{C_1}|\mathcal{H}_0}=\frac{1}{I_{\mathbf{F}}^{k+9}}\left(\frac{1}{I_{\mathbf{F}}^{k+9}}\left\|\tilde{\mathbf{F}}_{\mathbf{C}}^{k+9}\right\|_{l_1}^2-\hat{\mu}^2_{T_{\mathbf{F}}^{C_1}|\mathcal{H}_0}\right), \tag{47}$$

where the matrix $\tilde{\mathbf{F}}_{\mathbf{C}}^{k+9}$ can be expressed as

$$\tilde{\mathbf{F}}_{\mathbf{C}}^{k+9}=\mathbf{J_C}(k,k+9)\circ\mathbf{Z_C}(k,k+9). \tag{48}$$

In the second layer of the decision tree, to differentiate between SF3 and {SM,AL}, we construct the detection statistic as

$$T_{\mathbf{F}}^{C_2}=\frac{1}{L_{\mathbf{F}}^{k+2}}\left\|\mathbf{F}_{\mathbf{C}}^{k+2}\right\|_{l_1}, \tag{49}$$

where $L_{\mathbf{F}}^{k+2}$ represents the number of elements in matrix $\mathbf{F}_{\mathbf{C}}^{k+2}$, and matrix $\mathbf{F}_{\mathbf{C}}^{k+2}$ can be expressed as

$$\mathbf{F}_{\mathbf{C}}^{k+2}=\left[\mathbf{B_C}(4j-3,4j-1),\mathbf{B_C}(4j-2,4j)\right]^T. \tag{50}$$

The detection threshold $\Psi_{\mathbf{F}}^{C_2}$ for the second layer of the decision tree can be constructed as

$$\Psi_{\mathbf{F}}^{C_2}=Q_J\hat{\sigma}_{T_{\mathbf{F}}^{C_2}|\mathcal{H}_0}+\hat{\mu}_{T_{\mathbf{F}}^{C_2}|\mathcal{H}_0}, \tag{51}$$

where $\hat{\mu}_{T_{\mathbf{F}}^{C_2}|\mathcal{H}_0}$ can be represented as

$$\hat{\mu}_{T_{\mathbf{F}}^{C_2}|\mathcal{H}_0}=\frac{1}{I_{\mathbf{F}}^{k+5}}\left\|\tilde{\mathbf{F}}_{\mathbf{C}}^{k+5}\right\|_{l_1}, \tag{52}$$

in which $I_{\mathbf{F}}^{k+5}$ represents the number of elements in matrix $\tilde{\mathbf{F}}_{\mathbf{C}}^{k+5}$. Further, $\hat{\sigma}^2_{T_{\mathbf{F}}^{C_2}|\mathcal{H}_0}$ can be given as

$$\hat{\sigma}^2_{T_{\mathbf{F}}^{C_2}|\mathcal{H}_0}=\frac{1}{I_{\mathbf{F}}^{k+5}}\left(\frac{1}{I_{\mathbf{F}}^{k+5}}\left\|\tilde{\mathbf{F}}_{\mathbf{C}}^{k+5}\right\|_{F}^2-\hat{\mu}^2_{T_{\mathbf{F}}^{C_2}|\mathcal{H}_0}\right), \tag{53}$$

where the expression for $\tilde{\mathbf{F}}_{\mathbf{C}}^{k+5}$ is as

$$\tilde{\mathbf{F}}_{\mathbf{C}}^{k+5}=\mathbf{J_C}(k,k+5)\circ\mathbf{Z_C}(k,k+5). \tag{54}$$

In the final layer of the classification tree, AL and SM can be identified using the detection statistic $T_{\mathbf{F}}$ and the detection threshold $\Psi_{\mathbf{F}}$. Algorithm 1 gives the whole process of the proposed algorithm.

Algorithm 1 SFBCs recognition algorithm based on weighted cross correlation function.

1: Initialize the parameters b_0 and z_0;
2: Compute the weighted cross-correlation matrices $\mathbf{J_C}(k_1,k_2)$ and $\mathbf{Z_C}(k_1,k_2)$ of the received signals using (27) and (28);
3: Calculate the detection statistic $T_{\mathbf{F}}^{C_1}$ and the detection threshold $\Psi_{\mathbf{F}}^{C_1}$ using (42) and (45);
4: If $T_{\mathbf{F}}^{C_1}>\Psi_{\mathbf{F}}^{C_1}$, then classify the SFBC as SF4. Otherwise, proceed to step 5.
5: Calculate the detection statistic $T_{\mathbf{F}}^{C_2}$ and the detection threshold $\Psi_{\mathbf{F}}^{C_2}$ using (49) and (51);
6: If $T_{\mathbf{F}}^{C_2}>\Psi_{\mathbf{F}}^{C_2}$, then classify the spatial frequency encoding as SF3. Otherwise, proceed to step 7.
7: Calculate the detection statistic $T_{\mathbf{F}}$ and the detection threshold $\Psi_{\mathbf{F}}$ using (33) and (41);
8: If $T_{\mathbf{F}}>\Psi_{\mathbf{F}}$, then classify the spatial frequency encoding as AL. Otherwise, classify the spatial frequency mode as SM.

V. Simulation Results and Analysis

This section uses simulation to validate the performance of the proposed algorithm. In the examples, we consider a cognitive MIMO-OFDM system employing space-frequency block codes. The SFBCs scheme candidate pooling to be identified is $\Theta=\{\text{SM,AL,SF3,SF4}\}$. The simulation parameters are set as follows: the modulation scheme is QPSK, the number of subcarriers is $N_z=64$, the cyclic prefix length is $\nu=N_z/4$, the number of OFDM blocks is $N_b=100$, and the channel is set to a frequency-selective fading channel with $L_h=4$. The parameter factors b_0 and z_0 are initialized to 1.5 and 2. The detection factor $Q_{\mathbf{F}}$ is obtained using Monte Carlo. The characteristic exponent of the alpha-stable noise interference is $\alpha=1.5$. The signal-to-interference ratio in the simulation is defined as SIR $=10\lg(P_s/\gamma_\alpha)$, where P_s represents the total transmitted power and γ_α is the dispersion coefficient of the alpha-stable noise interference. The average recognition probability P_c is used to evaluate the performance of the recognition scheme, which is given by

$$P_c=\frac{1}{L_\Theta}\sum\mathrm{P}_r\left(\hat{C}_F\,|C_F\right) \tag{55}$$

where $C_F\in\Theta$ and L_Θ represents the number of elements in set Θ.

Fig. 3 shows the average recognition rate of the proposed method for different numbers of OFDM subcarriers N_z. In the simulation, the subcarrier numbers are set as $N_z=32$, $N_z=64$, and $N_z=128$, with SIR = 10dB. From Fig. 3, it can be observed that the recognition performance of the proposed algorithm improves as the number of OFDM subcarriers increases. When $N_z=32$ and SNR = - 7dB, the average recognition probability of the proposed algorithm is around 60%. However, when the number of OFDM subcarriers

$$\mathbf{F}_{\mathbf{C}}^{k+4}=\left[\mathbf{B_C}(8j-7,8j-3),\mathbf{B_C}(8j-6,8j-2),\ \mathbf{B_C}(8j-5,8j-1),\mathbf{B_C}(8j-4,8j)\right]^T \tag{43}$$

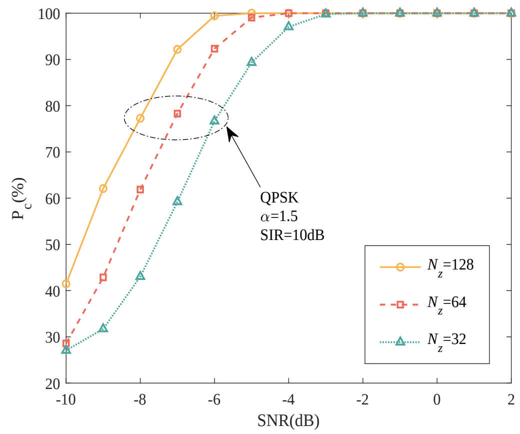

Fig. 3. Average probability of correct recognition versus SNR for different numbers of OFDM subcarriers.

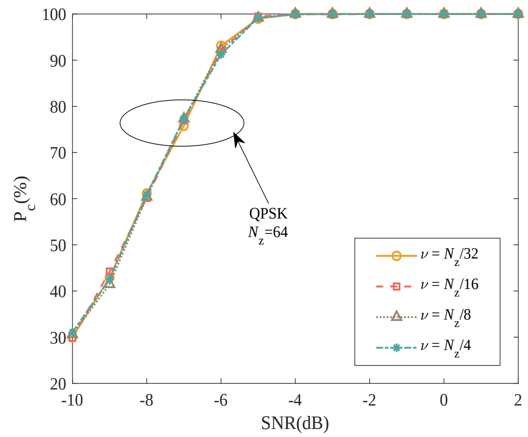

Fig. 5. Average probability of correct recognition versus SNR for different cyclic prefix length.

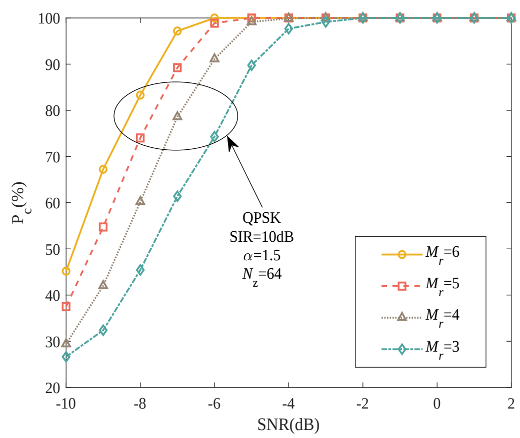

Fig. 4. Average probability of correct recognition versus SNR for different numbers of receive antennas.

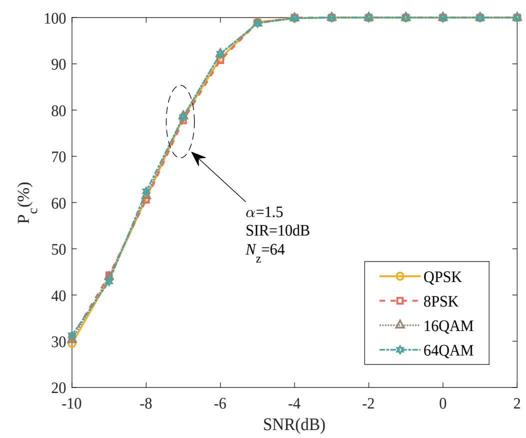

Fig. 6. The effect of the modulation type on the average probability of correct recognition versus SNR.

increases to $N_z = 128$, the average recognition probability exceeds 90%. This improvement is attributed to the increase in OFDM subcarriers, which causes the correlation between adjacent subcarriers to approach the theoretical value, thereby enhancing the distinguishability of different SFBC-OFDM schemes.

Fig. 4 shows the impact of the number of receiving antennas M_r on the average recognition probability. We consider the cases of $M_r = 4$, $M_r = 5$, $M_r = 6$, and $M_r = 7$, with SIR = 10dB. As shown in Fig. 4, the recognition performance of the proposed algorithm improves with an increase in the number of receiving antennas M_r. As M_r increases, the elements of the weighted cross-correlation feature matrix of the received signal also increase, causing the statistical measure to closer to the theoretical distribution and thereby enhancing the recognition performance.

Fig. 5 analyzes the influence of the OFDM cyclic prefix length ν on the recognition performance of the proposed algorithm. The cyclic prefix length of OFDM is set to $\nu = N_z/4$, $\nu = N_z/8$, $\nu = N_z/16$ and $\nu = N_z/32$, with SIR = 10dB. From Fig. 5, it can be observed that the average recognition probability of the proposed algorithm is not affected by the length of the OFDM cyclic prefix. This is because the proposed algorithm uses the demodulated OFDM signal to construct the recognition features, thereby eliminating the impact of the cyclic prefix.

Fig. 6 shows the average recognition probabilities under different modulation schemes. From Fig. 6, it can be observed that changing the modulation scheme does not affect the average recognition probability of the proposed algorithm. The proposed algorithm utilizes weighted cross-correlation features to construct the detection statistic and threshold. The modulation scheme does not contribute to the detection statistic and threshold. Therefore, it does not affect the recognition performance of the proposed method.

Fig. 7 illustrates the average recognition probabilities for different numbers of OFDM symbols. As illustrated in Fig. 7, the recognition accuracy of the proposed algorithm can be greatly improved with the increase in the number of OFDM symbols. This can be explained by the fact that the more significant features of the SFBC signal was exploited when the number of OFDM symbols were larger.

Fig. 8 shows the average recognition probabilities of the proposed algorithm under different SIRs. In the simulation

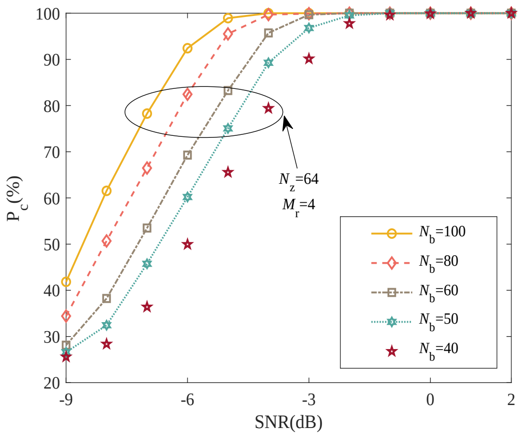

Fig. 7. Average probability of correct recognition versus SNR for different number of OFDM blocks.

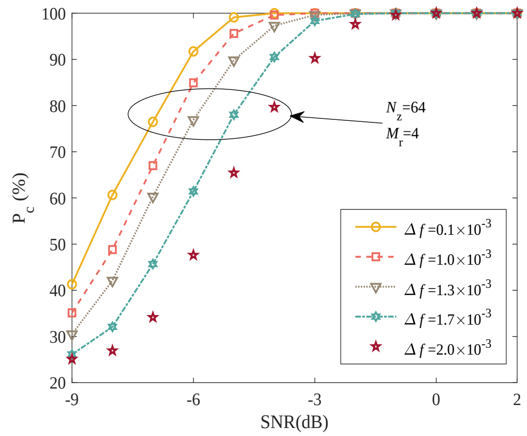

Fig. 9. The effect of the frequency offset on the average probability of correct recognition versus SNR.

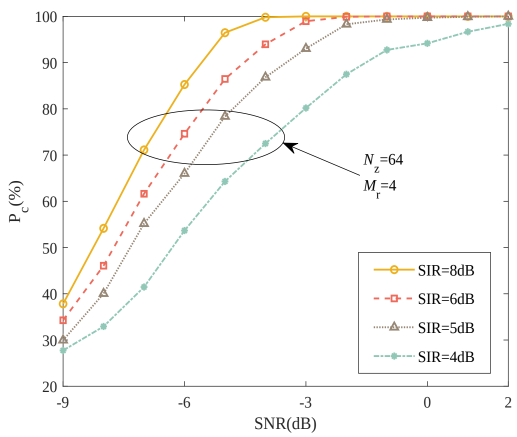

Fig. 8. The effect of the signal-to-interference ratio on the average probability of correct recognition versus SNR.

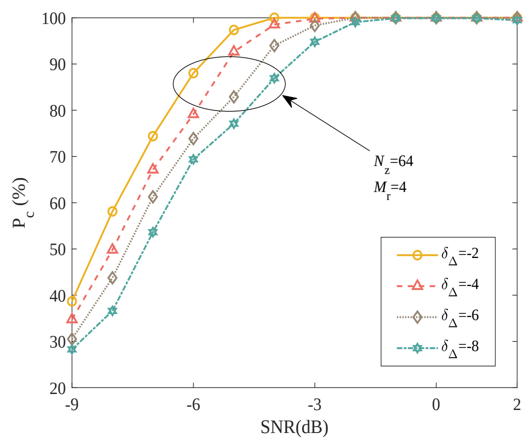

Fig. 10. The influence of the sample timing offset on the average probability of correct recognition.

experiments, we set $\alpha = 1.5$ and consider SIR $=$ 8dB, SIR $=$ 6dB, SIR $=$ 5dB and SIR $=$ 4dB. As shown in Fig. 8, the average recognition probability of the proposed algorithm increases with the SNR. When SIR $=$ 4dB and SNR = - 4dB, the average recognition probability of the proposed algorithm reaches around 70%. If the SIR is further increased to SIR $=$ 8dB, the average recognition probability approaches 99%. This is because as the SNR increases, the influence of non-Gaussian noise interference on the received signal decreases, resulting in greater correlation among adjacent subcarriers and improved recognition performance.

Fig. 9 examines the effect of the frequency offset Δf on the average recognition probability of the proposed algorithm. This example considers the normalized carrier frequency offset with respect to the sub-carrier spacing. As illustrated in Fig. 9, the performances improve considerably when the value of Δf decreases under the same conditions. When $\Delta f > 10^{-5}$, the performance degrades significantly. It concludes that the weighted cross-correlation function is not robust to the frequency offset.

Fig. 10 examines the effect of the the sample timing offset $\delta_{\triangle}$ on the average recognition probabilities of the proposed algorithm. As shown in Fig. 10, it can be seen that the rate of correct recognition increases of the proposed algorithm with a decrease in the sample timing offset $\delta_{\triangle}$. The simulation result indicates that the weighted cross-correlation function is sensitive to the sample timing offset $\delta_{\triangle}$. Especially, when $\delta_{\triangle} < -2$, the correlation properties of the weighted inter-correlation function are corrupted by $\delta_{\triangle}$, which leads to the degradation of the diversity of the recognition feature vectors, thus reducing the recognition performance of the SBCs scheme.

Fig. 11 shows the average recognition probability curves for different characteristic exponent α. A comparison with the algorithm based on the cross-correlation function (CCF) in [31] is also included. It can be observed from Fig. 11 that the recognition performance of the proposed algorithm decreases with α. When $\alpha = 1.4$ and SNR = - 5dB, the average recognition probability of the proposed algorithm is over 95%. However, when the characteristic exponent of alpha-stable interference is $\alpha = 1.1$, the average recognition probability drops to 50%. This is because a smaller characteristic exponent α corresponds to heavier tails of the non-Gaussian interference, indicating an increase in the number of

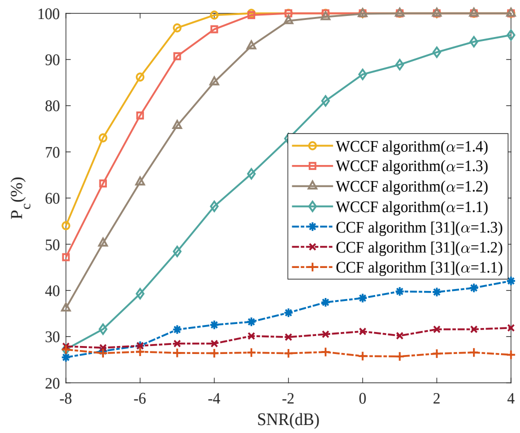

Fig. 11. The average probability of correct recognition of the SFBC-OFDM signals versus SNR, with different α values.

impulsive interferences in the received signal. These impulsive interferences disrupt the WCCF of the received signal, thereby affecting the recognition performance. In addition, the comparison of the recognition probability between the proposed WCCF algorithm and CCF algorithm is given for the same simulation conditions, which is shown in Fig. 11. The simulation results clearly indicate that the proposed WCCF algorithm outperforms the traditional CCF algorithm in terms of the recognition performance. Meanwhile, the computational complexities of WCCF algorithm and existing algorithms are evaluated. When the number of observed blocks and receive antennas are N_b and M_r, the calculation complexity for WCCF estimator is $O\left(3M_rN_b\right)$ and the CCF estimator also has order $O\left(M_rN_b\right)$.

VI. Conclusion

This paper has presented a recognition algorithm for SFBCs scheme in cognitive MIMO-OFDM systems, based on the weighted cross-correlation function. First, we analyzed the weighted cross-correlation function of the SFBC-OFDM signals. Then, we proposed a tree classification algorithm based on feature vectors to identify between several SFBCs under non-Gaussian impulsive interference. The proposed algorithm eliminated the need for preprocessing steps such as channel coefficient estimation, signal-to-noise ratio/signal-to-interference-plus-noise ratio estimation, and baseband modulation type recognition. The simulation results showed that the proposed algorithm effectively identifies SFBCs under non-Gaussian interference and frequency-selective fading. Furthermore, the algorithm exhibits favorable recognition performance in strong pulse interference environments and is unaffected by the baseband modulation type and the OFDM cyclic prefix length.

References

[1] F. Shen, Z. Wang, G. Ding, K. Li and Q. Wu, "3D compressed spectrum mapping with sampling locations optimization in spectrum-heterogeneous environment," *IEEE Trans. Wireless Commun.*, vol. 21, no. 1, pp. 326-338, Jan. 2022.

[2] H. Fang, T. Zhang, L. Zhang, H. Wu, G. Ding and Y. Cai, "Spectrum sensing under illegal spectrum access behaviors in multiple authorized users scenario," *IEEE Trans. Cogn. Commun. Netw*, vol. 7, no. 4, pp. 1186-1199, Dec. 2021.

[3] Z. An et al., "Series-constellation feature based blind modulation recognition for beyond 5G MIMO-OFDM systems with channel fading," *IEEE Trans. Cogn. Commun. Netw*, vol. 8, no. 2, pp. 793-811, Jun. 2022.

[4] D. Wang, F. Zhou, W. Lin, Z. Ding and N. Al-Dhahir, "Cooperative hybrid nonorthogonal multiple access-based mobile-edge computing in cognitive radio networks," *IEEE Trans. Cogn. Commun. Netw*, vol. 8, no. 2, pp. 1104-1117, Jun. 2022.

[5] A. Agrahari, P. Varshney and A. K. Jagannatham, "Precoding and downlink beamforming in multiuser MIMO-OFDM cognitive radio systems with spatial interference constraints," *IEEE Trans. Veh. Technol.*, vol. 67, no. 3, pp. 2289-2300, Mar. 2018.

[6] D. B. Rawat, "Evaluating performance of cognitive radio users in MIMO-OFDM-based wireless networks," *IEEE Wireless Commun. Lett.*, vol. 5, no. 5, pp. 476-479, Oct. 2016.

[7] P. Mertikopoulos and E. V. Belmega, "Transmit without regrets: online optimization in MIMO-OFDM cognitive radio systems," *IEEE J. Sel. Areas Commun.*, vol. 32, no. 11, pp. 1987-1999, Nov. 2014.

[8] X. Ge, X. Huang, Y. Wang, et al., "Energy-efficiency optimization for MIMO-OFDM mobile multimedia communication systems with QoS constraints," *IEEE Trans. Veh. Technol.*, vol. 63, no. 5, pp. 2127-2138, Jun. 2014.

[9] J. Tang, K. Cumanan and S. Lambotharan, "Sum-rate maximization technique for spectrum-sharing MIMO OFDM broadcast channels," *IEEE Trans. Veh. Technol.*, vol. 60, no. 4, pp. 1960-1964, May 2011.

[10] J. Liu and, K. Mei and X. Zhang, et al., "Fine timing and frequency synchronization for MIMO-OFDM: an extreme learning approach," *IEEE Trans. Cogn. Commun. Netw*, vol. 8, no. 2, pp. 720-732, Jun. 2022.

[11] K. Hamedani, L. Liu and Y. Yi, "Energy efficient MIMO-OFDM spectrum sensing using deep stacked spiking delayed feedback reservoir computing," *IEEE Trans. Green Commun. Netw.*, vol. 5, no. 1, pp. 484-496, Mar. 2021.

[12] M. Ghamari Adian and H. Aghaeinia, "Resource allocation in MIMO-OFDM-Based cooperative cognitive radio networks," *IEEE Trans. Commun.*, vol. 62, no. 7, pp. 2224-2235, Jul. 2014.

[13] A. Punchihewa, V. K. Bhargava and C. Despins, "Linear precoding for orthogonal space-time block coded MIMO-OFDM cognitive radio," *IEEE Trans. Commun.*, vol. 59, no. 3, pp. 767-779, Mar. 2020.

[14] V. Choqueuse, M. Marazin, L. Collin, K. C. Yao and G. Burel, "Blind recognition of linear space time block codes: a likelihood-based approach," *IEEE Trans. Signal Process.*, vol. 58, no. 3, pp. 1290-1299, Mar. 2010.

[15] Y. A. Eldemerdash, O. A. Dobre, M. Marey, G. K. Karagiannidis and B. Liao, "An efficient algorithm for space-time block code classification," in *Proc. IEEE Glob. Telecommun. Conf.*, 2013, pp. 3329-3334.

[16] V. Choqueuse, K. Yao, L. Collin and G. Burel,"Hierarchical space-time block code recognition using correlation matrices," *IEEE Trans. Wireless Commun.*, vol. 7, no. 9, pp. 3526-3534, Sep. 2008.

[17] G. Qian, L. Li, M. Luo, H. Liao and H. Zhang, "Blind recognition of space-time block code in MISO system," *EURASIP J. Wirel. Commun. Netw.*, 2013, pp. 1-12.

[18] Y. A. Eldemerdash, M. Marey, O. A. Dobre, G. K. Karagiannidis and R. Inkol, "Fourth-order statistics for blind classification of spatial multiplexing and Alamouti space-time block code signals," *IEEE Trans. Commun.*, vol. 61, no. 6, pp. 2420-2431, Jun. 2013.

[19] M. Marey, O. A. Dobre and B. Liao, "Classification of STBC systems over frequency-selective channels," *IEEE Trans. Veh. Technol.*, vol. 64, no. 4, pp. 2159-2164, May 2015.

[20] M. Shi, Y. Bar-Ness and W. Su, "STC and BLAST MIMO modulation recognition," in *Proc. IEEE Glob. Telecommun. Conf.*, 2007, pp. 3034-3039.

[21] C. Buiquang and T. Zhang, "Blind recognition of space time block code in MIMO systems," *Digit. Signal Process.*, vol. 83, pp. 1-5, Dec. 2018.

[22] M. R. DeYoung, R. W. Heath Jr. and B. L. Evans, "Using higher order cyclostationarity to identify space-time block codes," in *Proc. IEEE Glob. Telecommun. Conf.*, 2008, pp. 1-5.

[23] M. Marey, O. A. Dobre and R. Inkol, "Classification of space-time block codes based on second-order cyclostationarity with transmission impairments," *IEEE Trans. Wireless Commun.*, vol. 11, no. 7, pp. 2574-2584, Jul. 2012.

[24] M. Mohammadkarimi and O. A. Dobre, "Blind identification of spatial multiplexing and Alamouti space-time block code via Kolmogorov-

Smirnov (KS) test," *IEEE Commun. Lett.*, vol. 18, no. 10, pp. 1711-1714, Oct. 2014.

[25] M. Mohammadkarimi and O. A. Dobre, "A novel non-parametric method for blind identification of STBC codes," in *Proc. Can. Workshop Inf. Theory*, 2015, pp. 1-4.

[26] Y. A. Eldemerdash, O. A. Dobre and B. J. Liao, "Blind identification of SM and alamouti STBC-OFDM signals," *IEEE Trans. Wireless Commun.*, vol. 14, no. 2, pp. 972-982, Feb. 2015.

[27] E. Karami and O. A. Dobre, "Identification of SM-OFDM and AL-OFDM signals based on their second-order cyclostationarity," *IEEE Trans. Veh. Technol.*, vol. 64, no. 3, pp. 942-953, March 2015.

[28] M. Marey, O. A. Dobre and R. Inkol, "Blind STBC identification for multiple-antenna OFDM systems," *IEEE Trans. Commun.*, vol. 62, no. 5, pp. 1554-1567, May 2014.

[29] M. Marey and O. A. Dobre, "Automatic identification of space-frequency block coding for OFDM systems," *IEEE Trans. Wireless Commun.*, vol. 16, no. 1, pp. 117-128, Jan. 2017.

[30] M. Gao, Y. Li, O. A. Dobre and N. Al-Dhahir, "Blind identification of SFBC-OFDM signals using subspace decompositions and random matrix theory," *IEEE Trans. Veh. Technol.*, vol. 67, no. 10, pp. 9619-9630, Oct. 2018.

[31] M. Gao, Y. Li, O. A. Dobre and N. Al-Dhahir, "Blind identification of SFBC-OFDM signals based on the central limit theorem," *IEEE Trans. Wireless Commun.*, vol. 18, no. 7, pp. 3500-3514, Jul. 2019.

[32] J. Ma, M. Hu, T. Wang, Z. Yang, L. Wan, and T. Qiu, "Automatic modulation classification in impulsive noise: Hyperbolic-tangent cyclic spectrum and multibranch attention shuffle network," *IEEE Trans. Instrum. Meas.*, vol. 72, pp. 1-13, 2023.

[33] K. Hassan, R. Gautier, I. Dayoub, M. Berbineau and E. Radoi, "Multiple-antenna-based blind spectrum sensing in the presence of impulsive noise," *IEEE Trans. Veh. Technol.*, vol. 63, no. 5, pp. 4322-4339, Jun 2014.

[34] F. Moghimi, A. Nasri, and R. Schober, "Adaptive lp-norm spectrum sensing for cognitive radio networks," *IEEE Trans. Commun.*, vol. 59, no. 7, pp. 1934-1945, Jul. 2011.

[35] S. Kharbech, I. Dayoub, M. Zwingelstein-Colin and E. P. Simon, "Blind digital modulation identification for MIMO systems in railway environments with high-speed channels and impulsive noise," *IEEE Trans. Veh. Technol.*, vol. 67, no. 8, pp. 7370-7379, Aug. 2018.

[36] R. Barazideh, W. Sun, B. Natarajan, A. V. Nikitin, and Z. Wang, "Impulsive noise mitigation in underwater acoustic communication systems: experimental studies," in *Proc. IEEE 9th Annu. Comput. Commun. Workshop Conf.*, 2019, pp. 880-885.